

2025 | 161

## Development of an ammonia-fueled cracker-engine-unit as propulsion system for inland waterway vessel

Basic research & advanced engineering - new concepts

**Annalena Braun, Karlsruhe Institute of Technology**

Torsten Baufeld, Liebherr Machines Bulle  
Sören Bernhardt, Karlsruhe Institute of Technology  
Lena Engelmeier, ZBT - The Hydrogen and Fuel Cell Center  
Niklas Gierenz, University of Rostock  
Heiko Kubach, Karlsruhe Institute of Technology  
Hinrich Mohr, GasKraft Engineering  
Sascha Prehn, University of Rostock  
Sandro Silvestrini, Liebherr Machines Bulle

DOI: <https://doi.org/10.5281/zenodo.15191384>

---

This paper has been presented and published at the 31st CIMAC World Congress 2025 in Zürich, Switzerland. The CIMAC Congress is held every three years, each time in a different member country. The Congress program centres around the presentation of Technical Papers on engine research and development, application engineering on the original equipment side and engine operation and maintenance on the end-user side. The themes of the 2025 event included Digitalization & Connectivity for different applications, System Integration & Hybridization, Electrification & Fuel Cells Development, Emission Reduction Technologies, Conventional and New Fuels, Dual Fuel Engines, Lubricants, Product Development of Gas and Diesel Engines, Components & Tribology, Turbochargers, Controls & Automation, Engine Thermodynamics, Simulation Technologies as well as Basic Research & Advanced Engineering. The copyright of this paper is with CIMAC. For further information please visit <https://www.cimac.com>.

## ABSTRACT

The urgent need to reduce CO<sub>2</sub> emissions in all areas demands the swift development and implementation of appropriate solutions for the worldwide shipping branch both for sea-going and inland waterway vessels. Therefore, several options are viable, most of them based on green e-fuels. Ammonia, produced on basis of renewable energies e.g., by solar and wind power, looks as a promising candidate for shipping as worldwide trading and handling are already in place which eases the establishment of a fuel supply chain.

Within the CAMPFIRE alliance, new energy conversion and storage technologies based on green ammonia are investigated as part of the future energy systems. One of the projects focuses on the development of an ammonia-fueled cracker-engine-unit as propulsion system for inland waterway vessels. The spark-ignited heavy-duty engine will be fed by liquid ammonia as main fuel. A part stream of ammonia will be decomposed into hydrogen and nitrogen so that a small amount of hydrogen is brought to the engine as ignition amplifier for the ammonia. The project goal is the achievement of diesel-like engine output values with a maximum share of ammonia.

The paper describes the specific boundaries of inland waterway shipping, the ideas behind the monofuel propulsion concept and presents results from the pressurized ammonia cracker development as well as from the single-cylinder engine (SCE) testing. A further chapter will handle related safety experiences.

The ammonia cracker as automated stand-alone plant was developed according to the requirements set by the engine and on the basis of extensive catalyst testing as well as process and multi-physics simulations. Here, special emphasis is placed on challenges in the development process, e.g., the influence of the harsh conditions characterized by a combination of high temperature and ammonia-rich atmosphere on process and reactor design including the selection of a suitable material. The final cracker design is presented and first experimental results are discussed.

The SCE testing allowed a systematic investigation of various mixture formation concepts (PFI and DI) – supported by optical spray investigations -, different compression ratios and ignition systems. All that comes along with 3D-CFD simulations, especially for the mixture formation optimization. One important task was the development of fuel injectors suitable for liquid ammonia. During the whole SCE operation, a detailed emission measurement was carried out, enabling an extensive knowledge about the impact of various parameters.

The results will be transferred to the multi-cylinder engine, which is going to be married and tested with the ammonia cracker in 2025. Then specific focus will be set on the complete cracker-engine-unit optimization under maritime operational boundaries and the setup of an exhaust aftertreatment system.

## 1 INTRODUCTION

International trading relies in a big share on goods transport by ships. The respective CO<sub>2</sub> emissions are roughly like Germany's CO<sub>2</sub> emissions. These emissions need to be reduced similar to other industries. In this sense IMO (International Maritime Organization) has committed to achieve full climate neutrality for sea-going vessels until 2050 [1]. Inland waterway shipping must follow local regulations accordingly, e. g. by EU, EPA. In this respect ammonia is seen as an interesting fuel with carbon-free local combustion and its capability as hydrogen carrier with a worldwide existing supply chain network from the fertilizer industry.

Within the CAMPFIRE consortium several projects around energy conversion and storage of green ammonia as parts of future energy systems are ongoing [2]. One of these projects handles the development of a propulsion system for inland waterway vessels, based on pure ammonia as fuel. The main components of this system are an ammonia cracker, converting a part stream of the fuel input into hydrogen, and a high-speed engine fuelled by liquid ammonia and a small share of hydrogen as ignition amplifier. The interesting results of this development are presented in the following.

## 2 SYSTEM CONCEPT FOR AN INLAND WATERWAY VESSELS

The characteristic values of ammonia impact the volumetric and gravimetric storage capacity needs as well as the engine combustion concept engineering [3], combined with a suitable exhaust aftertreatment. Further challenges are material compatibility and lube oil interaction [4].

Within the CAMPFIRE project an existing ammonia tanker (MS ODIN) travelling mainly on river Rhine between Ludwigshafen/Germany and Rotterdam/The Netherlands was selected as test vessels for the later field testing of the propulsion system developed in the current project. Therefore, the existing direct drive diesel-fuel engine will be replaced by a hybrid drive system consisting of the ammonia-fuelled cracker and engine, a generator, battery, and electric propulsion engine connected to the propeller shaft as shown in Figure 1.

Recently, the typical operation and load profile of MS ODIN was recorded. The gained data are used on one hand for the layout of the hybrid system and on the other hand as basis for the upcoming cracker-engine testing at the CAMPFIRE facilities. Figure 2 shows an exemplary load graph from a lock passage of MS ODIN.



Figure 1. Scheme of propulsion of inland waterway vessel consisting of NH<sub>3</sub> tank, NH<sub>3</sub> cracker, combustion engine, generator, battery and propeller

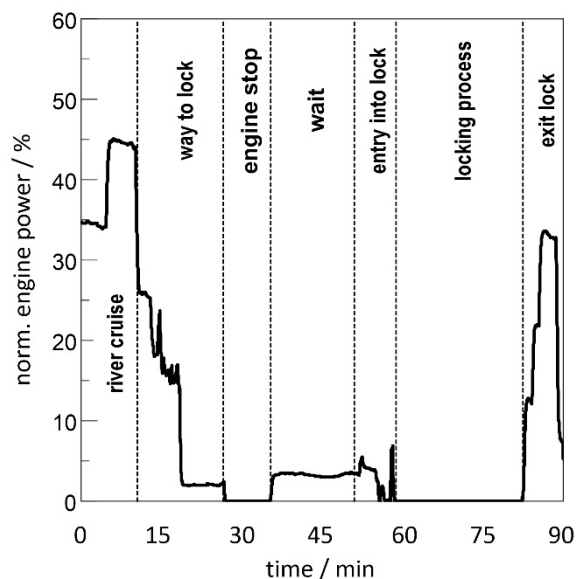


Figure 2. Engine power demand while locking process of MS ODIN

During the lock manoeuvre, the engine is operated at very low power for 60 minutes or the engine is completely stopped. This driving profile is basically well suited for a hybrid drive with a suitable battery design. On the one hand, operation can be carried out exclusively on battery power due to the low energy and power demand. On the other hand, the battery can alternatively be charged during the lock manoeuvre by increasing the engine and generator power. The latter also has advantages in terms of the requirements on the dynamics are reduced resulting in a longer service life among other things.

The power demand of inland water vessels is specifically lower compared to sea-going vessels due to lower speeds and less resistance by wind and waves. Only upriver routing leads to increased power demand, especially in areas with increased water flow velocities like gorge portions.

The typical installed propulsion power on a Europa type-vessel (85 m length, 9.5 m width) is 600 kW.

This allows a ship speed of nearly 10 knots in rivers and channels with a depth of 5 m. If the water level is reduced to e. g. 2.5 m, which can be observed currently in Europe quite regularly, the shallow water impact reduces the ship speed to approx. 5 knots using the same power than before. So, for future ship designs the shallow water operation need to be considered with regard to propulsion power and hull design [5].

The use of ammonia as a fuel also results in new requirements for ship design. Due to the hazardous substance classification of ammonia, e.g. on humans and living creatures as well as environmental hazards, adapted safety precautions must be implemented on the ship. All fuel pipes should be double-walled and equipped with pressure switches. In addition, the engine room and fuel storage room including the cracker system must be separated from other areas of the ship by at least two gas-tight walls and equipped with active ventilation. In addition, a gas warning sensor system must be provided to detect possible leaks at an early stage. If the gas warning system detects a leak of ammonia, the fuel lines are first divided into sections by tightly closing shut-off valves. This helps to minimise the amount of ammonia to the leaking section.

### 3 DEVELOPMENT METHODOLOGY

#### 3.1 NH<sub>3</sub>-Engine

If you look at the properties of ammonia compared to other fuels that are currently being discussed a lot in Table 1, you will notice that ammonia is very different. The high ignition temperature of 630 °C and the relatively small range of the volume fraction of ammonia in air in which ammonia actually burns shows that this fuel behaves significantly differently than hydrogen and methane.

When considering the concept, it quickly became clear that measures were needed that significantly supported both the ignition of ammonia and the rapid implementation of combustion. One advantageous concept that has now been published several times is diesel-fuel ignited and assisted NH<sub>3</sub> combustion. However, since CAMPFIRE favors completely CO<sub>2</sub>-neutral concepts, it was decided to use hydrogen as a carrier of ammonia, the combination of a very reactive fuel with a very inactive one. We will look at whether this combination also has disadvantages below. Several different concepts are now conceivable, which differ in the way in which ammonia and hydrogen are supplied to the engine as shown in Figure 3.

Table 1. Fuel properties [6,7]

Description	NH <sub>3</sub>	H <sub>2</sub>	diesel-fuel	CH <sub>4</sub> (LNG)
Lower Heating Value (MJ/kg)	18.6	120	42.7	46.4
Adiabatic flame temperature (°C)	1800	2110	2030	2000
Ignition temperature (°C)	630	560	>225	470
Evaporation energy (kJ/kg)	1368	223	200-300	511
Tank size compared to diesel-fuel	2.8	4.2	1	1.3

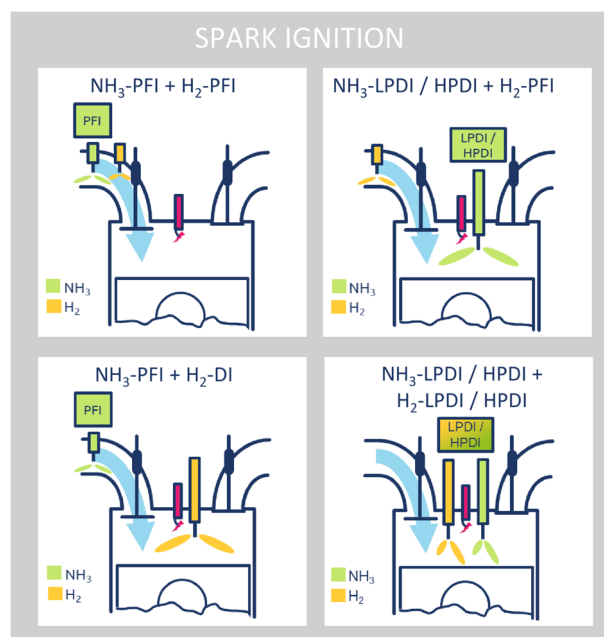


Figure 3. Overview of spark ignited (SI) combustion concepts with ammonia and hydrogen (promoter fuel). For direct injection, a differentiation is made between low-pressure (LP-DI) and high-pressure (HP-DI) fuel direct injection.

Both fuels can be blown into the intake manifold in front of the cylinder. Since a spark plug for ignition has to be placed as centrally as possible in the cylinder head, only one injector can inject directly into the cylinder due to space constraints. The second fuel has to be blown into the intake pipe quite close to the intake valve. However, since ammonia is already liquid at a temperature of 25°C and a pressure of around 10 bar, it is also possible to inject liquid ammonia, an approach that avoids the energy-intensive evaporation of the ammonia. It is also interesting to use the evaporative cooling of the ammonia to avoid knocking combustion of the hydrogen and, on the other hand, to intensify the ammonia combustion through higher compression. Chapter 4 presents some of the

combustion concepts investigated and also the test engine, a single-cylinder engine. These tests are intended to provide insights into the potential and performance of the different concepts in order to then move on to a 6-cylinder multi-cylinder engine with a selected concept and achieve further optimization. In general, the procedure was such that favorable operating parameters such as injection times and pressures for both ammonia and hydrogen were determined for each concept. In addition, the ignition timing was adjusted in each case. The engine speed was initially kept constant at 1500 rpm and then operating data was determined at the same load points. The criteria according to which the concepts are then evaluated are combustion stability ( $COV < 3$ ), fuel consumption, emissions (mainly  $NO_x$ ,  $N_2O$ ,  $CO$ ,  $NH_3$  and  $H_2$  slip) and the energetic share of  $H_2$  in relation to  $NH_3$ . The aim was to achieve a stable  $NH_3$  combustion with minimal  $H_2$  usage while maintaining a consistent  $H_2$  amount across the entire load range.

When selecting the combustion concept, aspects such as the performance of the injection components, especially for  $NH_3$ , and their potential to quickly achieve decent reliability were also considered. In addition, the potential for further optimizing combustion through improved mixture homogeneity, more optimal charge movement and better adapted piston geometries was also assessed. The further development of the 6-cylinder engine will begin in the second half of the year. The hydrogen for the 6-cylinder engine will then be supplied by a cracker that produces  $H_2$  and  $N_2$  directly from  $NH_3$ . The developments of this cracker are currently running in parallel and are presented below.

### 3.2 Cracker

In order to supply the required amount of hydrogen to the engine, a portion of the ammonia feed has to be decomposed into hydrogen in an ammonia cracker. Despite numerous research and development activities, ammonia cracker are not yet state of the art, are therefore not yet commercially available and must be developed according to the specific application requirements. The main requirements set by the engine are summarized in Table 2. At full engine load, the cracker must supply 4,5 kg/h of hydrogen, equivalent to 150 kWh<sub>2</sub>, meeting up to 17 % of the engine's total energy demand. The basis of the cracker development is the identification and selection of a suitable catalyst for the decomposition of ammonia into hydrogen, Nitrogen and residual ammonia. Therefore, various catalysts are extensively tested regarding their conversion depending on temperature, pressure, educt volume flow and long-term stability.

Table 2. Boundary conditions for the development of the ammonia cracker

Description	Value
Energy content of hydrogen in the engine fuel	Up to 17 %
hydrogen power of the cracker product gas	150 kW
Cracker product gas pressure	6-8 bar
Cracker product gas temperature	< 60 °C
Residual ammonia content of the cracker product gas	$x_{NH_3} < 5 \text{ mol } \%$

The most suitable catalyst is selected and an application-oriented microkinetic approach is determined. Based on the physical and chemical properties, geometry and activity of the catalyst as well as the requirements set by the engine the ammonia cracker is designed, focusing on an optimized heat integration and thus high efficiency.

A zero-dimensional (0D) process simulation tool is employed to model and compare different process designs and finally to determine energy and material flows essential for designing the ammonia cracker components such as the reactor and heat exchangers. The detailed engineering of these components is supported by Multiphysics simulations as well as finite element methods.

The engineering and construction of the entire ammonia cracking plant, which, in addition to the designed cracker module (consisting of cracker reactor, heat exchangers, piping, instrumentation and insulation), includes the balance-of-plant components, mainly actuators and sensors, as well as safety technology, the rack and the control system (SPS) for automated operation. The developed ammonia cracking plant is commissioned and undergoes systematic testing and optimization. The cracking plant will then be integrated in a standard container and coupled with the packaged genset for extensive testing of the entire system. Both the initial operation as well as the subsequent tests with the genset will be used for process optimization supported by a digital twin with dynamic process simulation.

### 3.3 Internal Combustion Engine

The development of a suitable engine concept for a multi-cylinder engine was initially carried out on a single-cylinder research engine as shown in Figure 4. Optical measurement technology was used to analyze the spray behavior of the injector and validate a 3D CFD model for injection and mixture formation. A 0D/1D model was also created for combustion analysis and simulation. Extensive parameter variations were then carried out using

different configurations and compression ratios. Based on the results obtained, a concept with intake manifold injection of liquid ammonia and gaseous hydrogen and a compression ratio of 18.5 was favored [3]. Various options for igniting ammonia-hydrogen mixtures with the lowest possible hydrogen content are discussed in the following chapters.

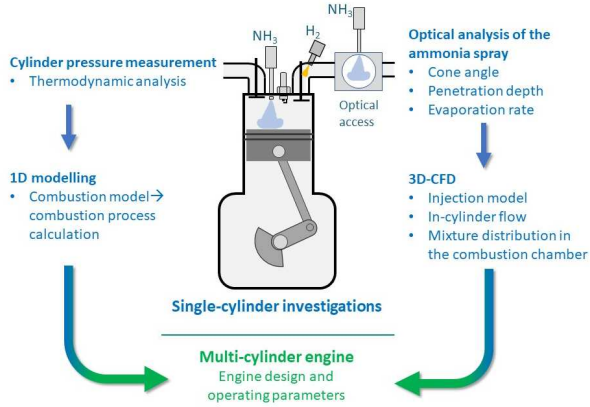


Figure 4. Development methodology of the combustion process for the multi-cylinder-engine

## 4 RESULTS

### 4.1 0D/1D Simulation

A 0D/1D-simulation model was also developed within this project in order to be able to model the ammonia-hydrogen combustion process. The commercial software GT-SUITE was used to achieve this goal. Due to the spark-ignited combustion and the homogeneous mixed charge the SI-Turb model was chosen for this task. This model is often chosen in literature for the simulation of gasoline or hydrogen SI-engines. It is a two-zone combustion model where the heat-release rate is simulated by a turbulent propagating flame. This flame is assumed spherical whereby the flame wrinkling effect is captured by a turbulent flame speed. This turbulent flame speed is added to the laminar flame speed which needs to be calculated in respect to the mixture and its thermodynamic properties, like temperature, pressure and air-fuel-ratio.

The entrained mass rate of the unburned air-fuel mixture is captured by formula (1):

$$\frac{dM_e}{dt} = \rho_u A_f (S_T + S_L) \quad (1)$$

Where is  $\rho_u$  the density of the unburned zone,  $A_f$  the flame area,  $S_T$  the turbulent flame speed and  $S_L$  the laminar flame speed.

While for conventional fuels and pure hydrogen-air- or ammonia-air-mixtures the calculation of  $S_L$  is implemented in the used 0D/1D-software, in this work the calculation for the investigated hydrogen-ammonia-air-mixture needed the implementation of external literature work from [8]. After integrating the validated formulas for calculating the laminar flame speed for given hydrogen-ammonia ratios and thermodynamic properties in engine-relevant conditions the further needed calibration multipliers of the turbulent flame speed model could be applied by matching the calculated heat release with experimental data.

Table 3. Engine conditions for 0D/1D simulation model

Parameter	Lower limit	Upper limit
Engine speed in rpm	1300	1800
Charge air pressure in bar	1.3	2.4
Lambda	0.9	2.4
Energetic NH <sub>3</sub> -content in %	0	88

To achieve this, a method needs to be applied which is called Three-Pressure-Analysis (TPA). With this TPA model the measured air flow and the exhaust gas temperatures can be compared and if necessary matched with the help of additional multipliers. Figure 5 shows the results of the TPA analysis after model calibration. The deviation of volumetric efficiency is met within a 5 % span. The temperature after cylinder is computed with errors of 30 Kelvin.

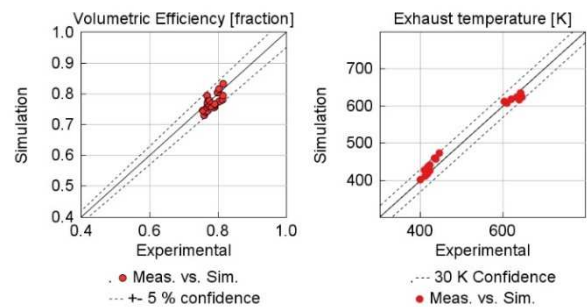


Figure 5. Comparison of experimental and simulation results regarding volumetric efficiency and exhaust temperature

This seems to be satisfactory especially considering the data set spans a wide variety of conditions as shown in Table 3. After ensuring that the measuring points of the TPA were sufficient, the calibration of the above-mentioned multipliers in the combustion model could now be continued.

A selection of the resulting pressure and burn rate traces are shown in Figure 6. Generally, a sufficient comparison between the measured and predicted results can be observed. In conditions with a high energetic share of ammonia (>80 %) and lambda values between 0.9 and 1.5 the best results could be achieved.

Concerning low ammonia shares and high lambda values (>1.5) the model shows some uncertainties.

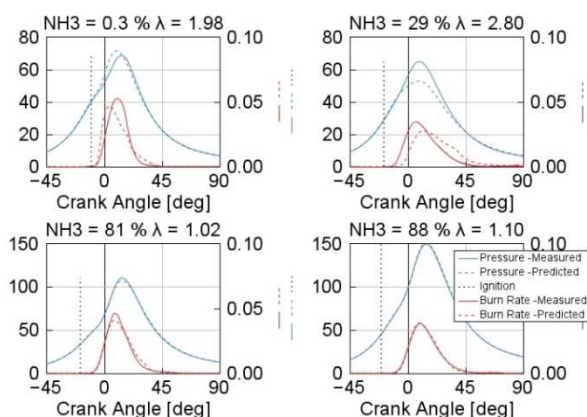


Figure 6. Selection of pressure and heat traces of the calibrated combustion model.

While in the case with almost 100 % hydrogen the burn rate is predicted to be too steep, which results in higher pressures than measured, in the most cases with a low and medium hydrogen content the predicted pressure tends to be lower than measured. This is caused by a much slower burn rate than measured. These uncertainties could be minimised by reducing the experimental space to a reasonable size for later application. Also, an improvement is needed regarding the evaporation model of the ammonia-port-injector. After those improvements this model can be used to support the development of the multi-cylinder engine regarding turbocharger matching and investigations of useful control strategies.

## 4.2 CFD Simulation

In addition to the 1D simulation the 3D CFD simulation gives a better understanding of the mixture formation and possible optimisations regarding injector position. This study investigates, using computational fluid dynamics (CFD) models based on experimental data and existing literature, the application of direct liquid ammonia injection and port fuel hydrogen injection technologies in a SI engine. The primary objective of this analysis is to gain a deeper understanding of how the mixture formation and combustion propagation are influenced by various parameters, including injection timing, injection pressure, piston shape,

injection position, and injection direction. The aim is to identify the optimal trade-offs for these factors.

A significant challenge in the case under investigation is simulating ammonia evaporation at low injection pressures. This difficulty arises due to the limited understanding of evaporation behavior under these specific injection conditions. To address this, the study employs a validated evaporation model sourced from literature [11]. Once the model was validated, the amount of liquid ammonia actually participating in combustion was determined from average measurements. This step is crucial, as it provides the necessary data to verify the accuracy of the simulation. The engine model was divided into two distinct simulations: a Volume of Fluid (VoF) simulation of the injector, designed to capture ammonia behavior at the nozzle outlet, and an engine simulation utilizing a Lagrangian spray configuration, based on the VoF results and the validated evaporation model. This combined approach produced results that closely matched experimental measurements from simulations at low injection pressures, as shown in Figure 7.

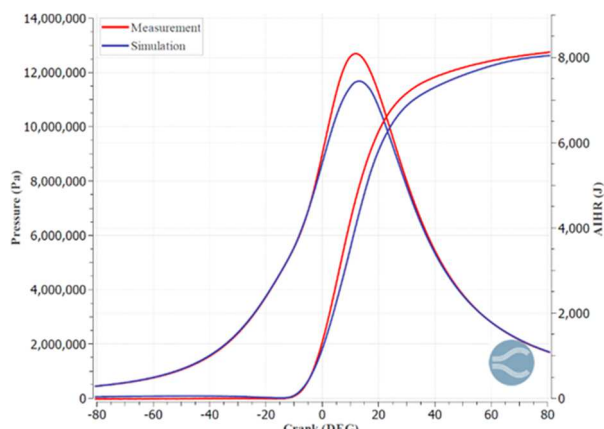


Figure 7. Cylinder pressure and apparent heat release comparison

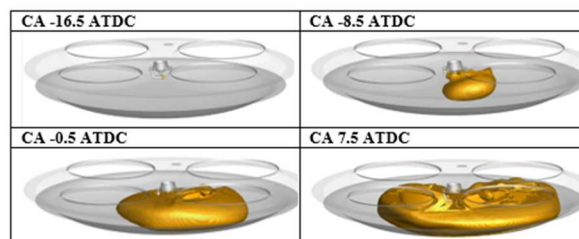


Figure 8. Hydrogen-ammonia combustion propagation

The slower combustion propagation and the reduced in-cylinder peak pressure will be subject to further investigation in the subsequent stages of this study. The 3D simulation results provide a more comprehensive understanding of the behavior within the combustion chamber. For

instance, it was concluded that in the case of low injection pressure analyzed, the  $\text{NH}_3\text{-H}_2$  mixture exhibits homogeneous combustion propagation originating from the spark plug. This behavior is illustrated in the following Figure 8, through the temperature ISO-surfaces.

### 4.3 Combustion Process Development on the Single-Cylinder Engine

In the next chapter, the combustion process results on the single-cylinder engine are examined. These results form the basis for the design and operating strategy of the multi-cylinder engine.

#### 4.3.1 Testbed and Single-Cylinder Engine

The test engine is a single-cylinder engine based on the Liebherr D966 diesel-fuel engine. To allow proper single-cylinder engine monitoring and data acquisition of a wide range of relevant information for engine testing, the experimental activities were carried out in a fully instrumented testbench, as depicted in Figure 9. The cylinder head was modified so that a sleeve with spark plug can be fitted in place of the diesel-fuel injector. A specially manufactured intake manifold can accommodate both an injector for hydrogen and an ammonia injector. The relevant engine data are listed in Table 4.

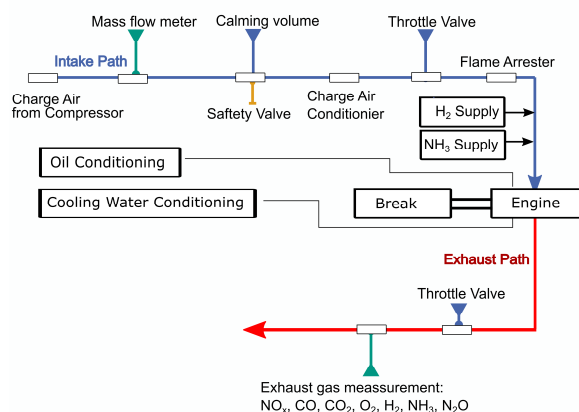


Figure 9. Scheme of the single-cylinder engine testbench

The engine was coupled to a dynamometer to control load and speed. The in-cylinder pressure was measured by a piezoelectric pressure transducer in conjunction with a piezo charge amplifier and referenced by an encoder with a resolution of 0.1 crank-angle degrees. Absolute piezo pressure sensors were used to measure the intake pressure, exhaust pressure and fuel pressure of the ammonia. The ignition settings were controlled by a default ignition system. All the sensors above were connected to a high-speed data acquisition unit, allowing real-time combustion

analysis. Quantitative information about the combustion process and its cycle-to-cycle variability was obtained through a heat-release analysis from 100 consecutive cycles.

The fuel mass was measured by a coriolis mass flowmeter. The air mass was measured by a rotary piston meter. A wide-band lambda sensor LSU 4.9, conditioned by a Lambda Meter, determined the exhaust oxygen concentration. This allows the calculation of the air-fuel ratio. The concentration of  $\text{CO}_2$ ,  $\text{O}_2$  and  $\text{NO}_x$  on the exhaust were measured through a default exhaust gas measurement system. The concentration of  $\text{NH}_3$ ,  $\text{N}_2\text{O}$  and  $\text{NO}_x$  on the exhaust were measured by a FTIR and the  $\text{H}_2$  in the exhaust was measured by a mass spectrometer based on the principle of electron impact ionisation.

Table 4. Single-cylinder engine data

Engine	Detail
Stroke	157 mm
Bore	135 mm
Max. Speed	1900 rpm
Operation principle	4-stroke SI
Displacement	2.24 l
Compression Ratio	18.5
Type	Modified Liebherr diesel-fuel engine based on D966

#### 4.3.2 Injection System Configuration

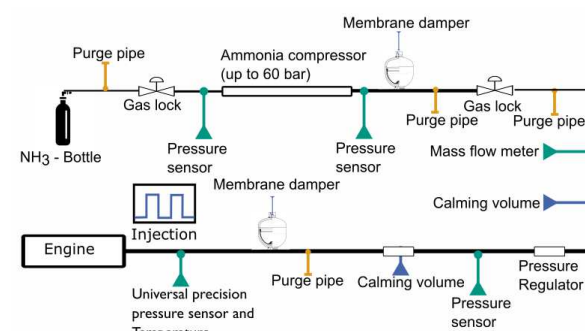


Figure 10. Principle sketch of the ammonia infrastructure

The engine is equipped with three different fuel infrastructures (ammonia, hydrogen and diesel-fuel). Ammonia and hydrogen were supplied from storage bottles. Hydrogen is supplied in gaseous phase at a pressure of 300 bar at ambient temperature and can therefore be injected directly into the intake manifold via a pressure reducer. Most of the  $\text{NH}_3$  is in liquid form in the ammonia storage bottles. The ammonia pressure is a function of the ambient temperature via the vapour

pressure in the bottles and is in the range of 2 to 8 bar. To achieve the desired injection pressure the  $\text{NH}_3$  must be compressed. For this purpose, a double-acting compressor station was integrated, which can compress liquid and gaseous  $\text{NH}_3$  up to 60 bar. The ammonia injector can be operated up to a pressure of 30 bar. In order to avoid pressure pulsations in the injection path, two membrane dampers and two calming volumes were integrated into the injection pipes. The basic structure of the  $\text{NH}_3$  supply system is shown in Figure 10.

#### 4.4 Combustion Process Development

The present study is divided in three sections. The first section explores the influence of different ignition concepts to maximize the energetic ammonia share for a SI combustion process. The second chapter explores the differences between a 100 % ammonia combustion and a hydrogen-ammonia combustion. The third section compares a SI ammonia-hydrogen combustion with a diesel-fuel-ammonia combustion.

##### 4.4.1 Variation of the Ignition System

The first chapter explores the influence of different ignition concepts. The goal of the combustion concept development is to run the engine with as high as possible energetic  $\text{NH}_3$  share. The cracker can thus be dimensioned as small as possible or left out. There are several approaches to achieve this goal. As the CAMPFIRE results at RGMT 2024 [3] have shown the main fact to get a stable ammonia combustion is to improve the ignition energy. The ignition energy and ignition phase are decisive factors for good combustion with low cyclical fluctuations. The cyclic fluctuations can be reduced via hydrogen, via a high energy ignition system or a pre-chamber spark plug. The configuration of the engine for this measurement was ammonia (liquid) and hydrogen (gaseous) via PFI as shown in Figure 11. The charge air measuring point is before these two injections. In this chapter these three options will be compared at several load points. The global lambda is set to 1 for every configuration. The goal is a COV of IMEP below 3%, the exhaust gas temperature must not exceed 650 °C and the peak pressure must not exceed 200 bar.

In Figure 12 the passive pre-chamber sparkplug is completely mounted in the cylinder head. In the pre-chamber a J-gap spark plug is mounted. The goal is to create a turbulent jet of hot gas that improves the ignition of the main fuel-air mixture. It could ensure a more complete combustion with regard on the emissions. The charge air temperature is set to 60 °C.

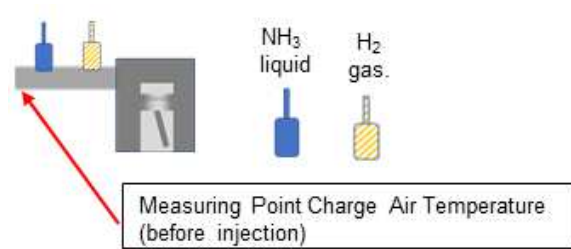


Figure 11. Principle sketch of the engine assembly with hydrogen and ammonia injector position

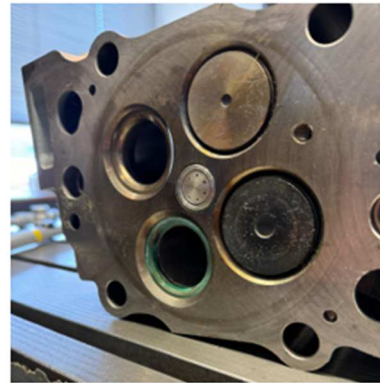


Figure 12. Pre-chamber sparkplug mounted in the cylinder head

The third option is a suitable ignition system. A high energy capacitive ignition system was used for this purpose. This has the possibility to adjust the spark duration and the spark current variably. The longer duration of the spark over several degrees of crank angle increases the probability that ignitable mixture will flow past the spark plug and ignite as shown in Figure 13.

With this capacitive ignition system, the ignition spark voltage, the ignition spark burning time and the ignition spark holding current can be variably adjusted. The high energy ignition system recognizes when a spark fails, then the capacitor discharge is switched off and the current is regulated by the plasma to a target value until it is switched off after a set time interval. This always triggers a spark and eliminates the excess current, which reduces spark plug wear [9].

The current is set in the closed control loop to values in 50 to 200 mA and the duration in 40 to 3000  $\mu\text{s}$ , which leads to spark energies in 2 to 150 mJ. This capacitive ignition system does not necessarily lead to increased wear of the spark plug. With a suitable choice of current and control duration, the ignition spark can be maintained in the low-wear glow discharge.

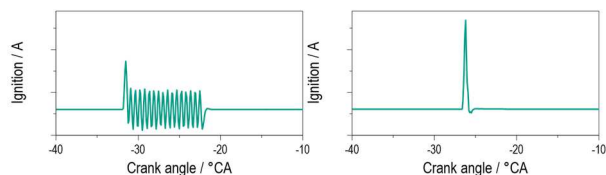


Figure 13. Ignition signal measured on the primary side with a current clamp. Left: Capacitive high energy system. Right: Default inductive system

Figure 14 shows the restriction of the different ignition concepts. The energetic  $\text{NH}_3$  share is plotted vs. the IMEP. With the default ignition system (green) the highest energetic  $\text{NH}_3$  share of 89 % can be achieved at full load which means 22 bar IMEP. In lower load points less energetic  $\text{NH}_3$  share can be achieved. At higher energetic ammonia shares the combustion gets unstable which means a COV of IMEP over 3 %.

The passive pre-chamber spark plug shows a better performance. The maximum energetic  $\text{NH}_3$  share is 100 % at full load. In lower load points it is not possible to run the engine without hydrogen. At least 10 % energetic hydrogen share is always necessary except for the full load. It can be seen in Figure 14 that the high energy ignition system enables a 100 % ammonia combustion in almost every load point. Even the possible range of  $\text{NH}_3$  and  $\text{H}_2$  share is wider than with the other ignition systems. In low load points at 2 bar IMEP, which means idle load, an energetic  $\text{NH}_3$  share of 60 % is possible. With this system the Cracker is most necessary at low load points. In load points of 6 bar IMEP and higher the engine can be operated without hydrogen and 100 % ammonia.

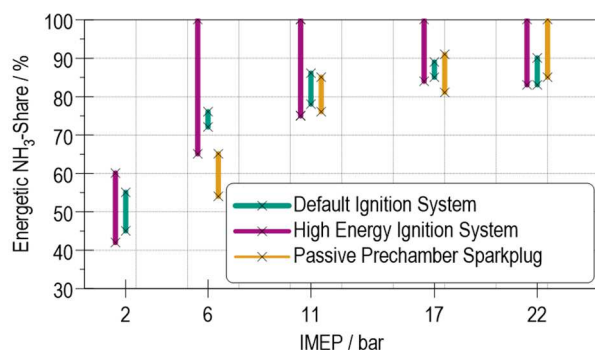


Figure 14. Restriction of the different ignition concepts.

As shown in Figure 15 the indicated efficiency is very similar for all ignition concepts and on a level of 50 % at full load conditions. It rises in a comparable way with increasing load. There is also no big difference in the peak pressure and exhaust gas temperature for the different ignition concepts. At full load the peak pressure is for all ignition

concepts close to 200 bar which must not be exceeded in this engine.

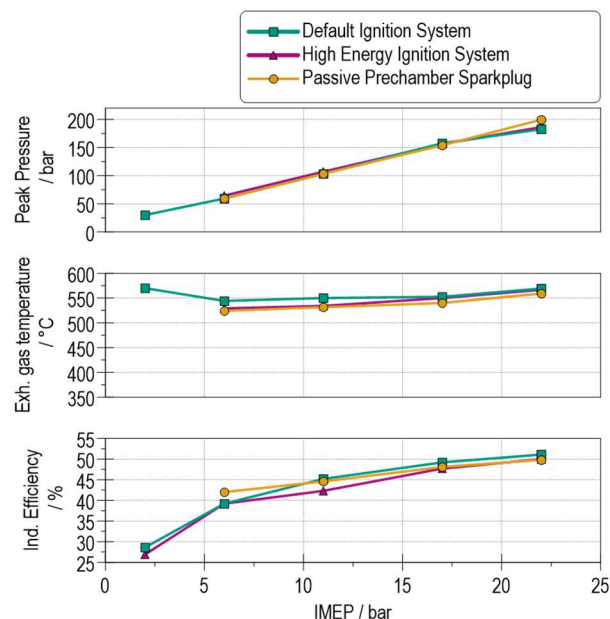


Figure 15. Peak pressure, exhaust gas temperature and indicated efficiency for different load points depending on the ignition system

In Figure 16 the ignition timing, mfb 10%, mfb 50%, mfb 90% and the energetic  $\text{NH}_3$  share are plotted vs. the IMEP. The mfb 50% was kept to 8 °CA aTDC for all load points except for the full load. The compression ratio of 18.5 leads to an exceed of the peak pressure (200 bar) so the mfb 50% has to be set later. Although the mfb 50% is similar for the three ignition concepts the mfb 90% differs. The small amount of  $\text{H}_2$  which is needed for the default ignition system leads to a quicker end of the combustion process. The passive Pre-Chamber sparkplug takes a longer time to burn 90 % of the fuel mass.

The burning delay increases for the high energy ignition system. That means the time to start the combustion takes longer due to a lower laminar flame speed of the pure ammonia. Figure 17 shows the burning delay and the burning time over the IMEP.

At 17 bar IMEP and maximum energetic  $\text{NH}_3$  share the cyclic fluctuations of the high energy ignition system (Figure 18 red) are lower than with the other ignition concepts as shown in Figure 18. The horizontal dispersion of the default ignition concept shows that there is no correlation between the ignition timing and the burn-through phase. For example, there are green points at -8 °CA mfb 10% and 31 °CA mfb 90% and there are also points at -1 °CA mfb 10% and 31 °CA mfb 90%. The flat

gradient shows that a later mfb 10% does imply a later mfb 90% for the mean value.

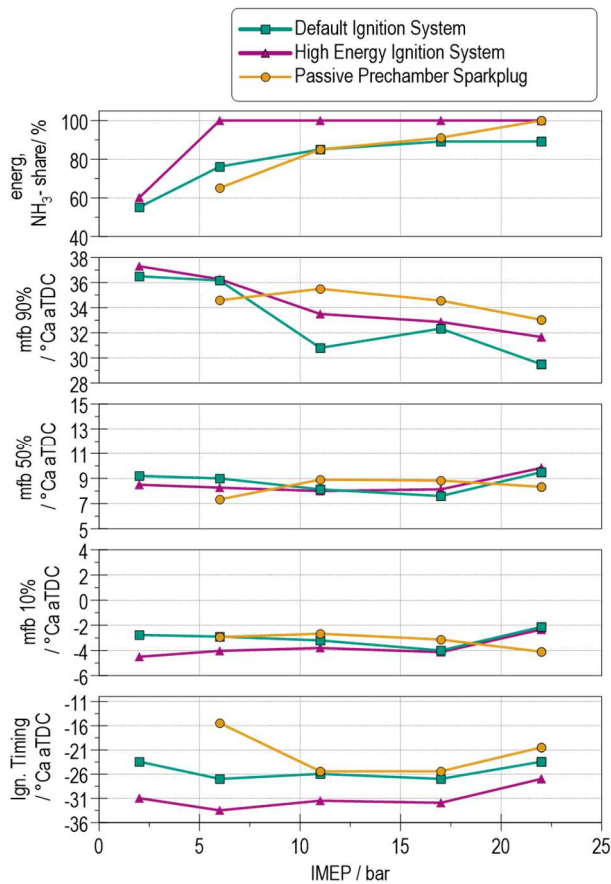


Figure 16. Energetic NH<sub>3</sub> share, mfb 90, mfb 50, mfb 10 and ignition timing for different load points depending on the ignition concepts.

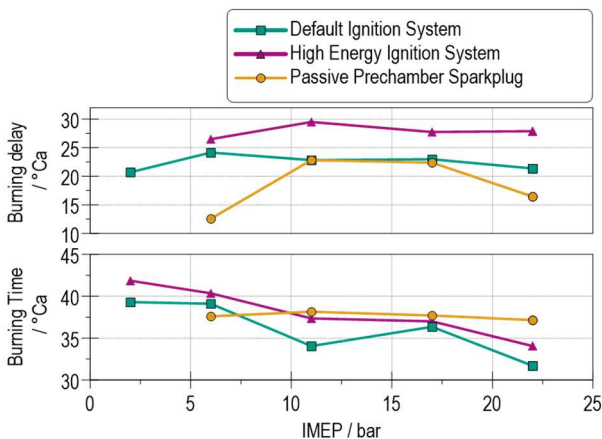


Figure 17. Burning delay and burning time over the IMEP for different ignition concepts

Figure 19 shows the total heating value and the net heat release rate for the three different ignition concepts at 17 bar IMEP and maximum energetic NH<sub>3</sub> share. These are the mean values of each measurement with the lowest COV of IMEP to

compare the duration of the combustion. The high energy ignition system has a comparable combustion duration to the default ignition system. Although there is hydrogen needed with the default system. The jets which are coming out of the passive pre-chamber spark plug produce a higher activated volume. The combustion is quicker at the beginning but then the combustion duration decreases, and the combustion process is similar to the other ignition concepts.

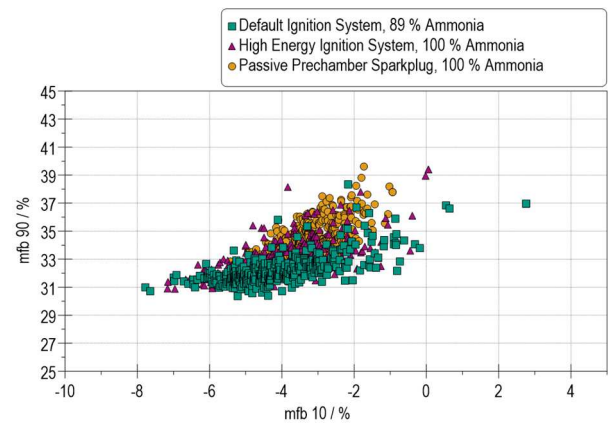


Figure 18. Comparison of mfb 90% and mfb 10% for the default ign. system, the high energy ign. system and the pre-chamber spark plug at 17 bar IMEP, lambda 1 and the maximum possible energetic NH<sub>3</sub> share

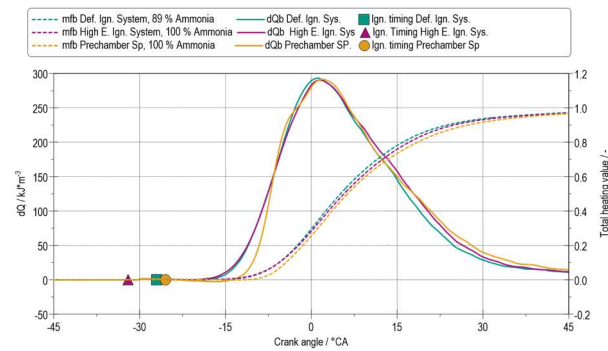


Figure 19. Total heating value, net heat release rate and ignition timing over crank angle for three different Ignition concepts at 17 bar IMEP, lambda 1

Figure 20 shows the NO<sub>x</sub>, NH<sub>3</sub>, N<sub>2</sub>O and H<sub>2</sub> emissions over the energetic NH<sub>3</sub> share at 17 bar IMEP for the different ignition concepts. The NO<sub>x</sub> emissions are in a range of 5-12 g/kWh. The passive pre-chamber spark plug is on a similar range than the other ignition concepts even though it can usually decrease the NO<sub>x</sub> emissions in common pre-chamber combustion processes. The difference is that it usually enables an operation with leaner air-fuel mixtures which decreases the in-cylinder temperature and with that the NO<sub>x</sub>

emissions. In this combustion process  $\text{NO}_x$  can not only be produced by the Zeldovic mechanism but it can be produced out of the fuel itself. The laughing gas emissions ( $\text{N}_2\text{O}$ ) are quite low and potentials for further reduction are seen.

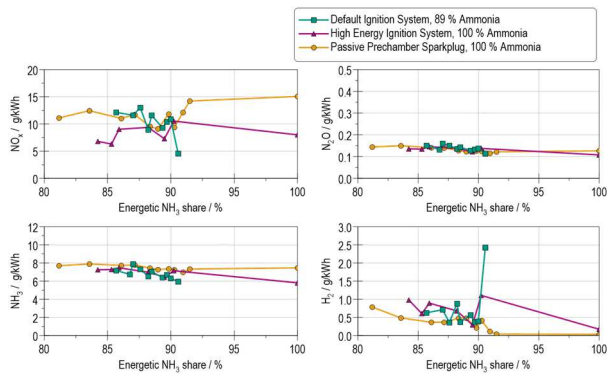


Figure 20. Emissions over the energetic  $\text{NH}_3$  share for different ignition concepts at 17 bar IMEP and  $\lambda$  1

Summing up it can be said for all ignition concepts a higher load point leads to an increase of the possible energetic  $\text{NH}_3$  share. This is due to the higher in cylinder temperatures and pressures which improve the ammonia combustion process. The main factor for a stable combustion is to improve the start of the ammonia combustion process. Once there is enough energy to initial ignite the pure ammonia it will burn as fast as a hydrogen-ammonia mixture. The measurements have also shown that even at lower load points the combustion can be significantly improved by a high energy ignition system.

#### 4.4.2 Pure Ammonia Combustion vs. Ammonia-Hydrogen Combustion

In this chapter a 100 % ammonia combustion will be compared to a hydrogen-ammonia combustion process. The engine was equipped with a hydrogen and an ammonia injector in PFI mode as shown in Figure 11. For the 100 % ammonia experiments the hydrogen injector was turned off and the high energy ignition system was mounted. Due to the slower laminar flame speed of ammonia, one could assume that the combustion process is significantly slower in 100 % ammonia operation compared to a hydrogen-ammonia combustion. Which would result in a reduction in efficiency.

Figure 21 shows the total heating value and the net heat release rate for both combustion processes. For the 100 % ammonia combustion, the ignition timing must be set significantly earlier to reach the same mfb 50%. Once combustion has started, there is not much difference in the combustion processes. The end of combustion is also around 30 °CA aTDC. This means that 100% ammonia

combustion is bit slower than the combustion of a hydrogen-ammonia mixture. The high energy ignition system is able to start the combustion process and thus the 100 % ammonia decomposes into hydrogen and nitrogen. The decomposition causes the combustion of pure ammonia to take place just as quickly as with an ammonia-hydrogen mixture, despite the significantly slower laminar flame speed of the ammonia.

Figure 22 shows the cylinder pressure for a 100 % ammonia combustion and a hydrogen-ammonia combustion at 17 bar IMEP which means 75 % load. The grey lines show 100 measured cycles and the coloured line is the mean value of the 100 cycles. Figure 22 left shows the hydrogen-ammonia combustion with 85 % energetic ammonia share. Figure 22 right shows a 100 % ammonia combustion. It can be observed that the peak pressure is slightly higher when hydrogen is injected. A slight knocking can be seen on the left-hand side. The 100 % ammonia combustion does not tend to knocking although the ammonia decomposes into hydrogen and nitrogen during the combustion process. The hydrogen is created out of the ammonia after the flame front.

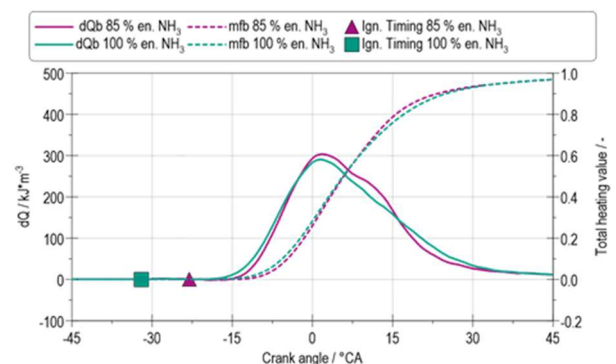


Figure 21. Total heating value, net heat release rate and ignition timing over crank angle for hydrogen-ammonia and 100 % ammonia at 17 bar IMEP,  $\lambda$  1

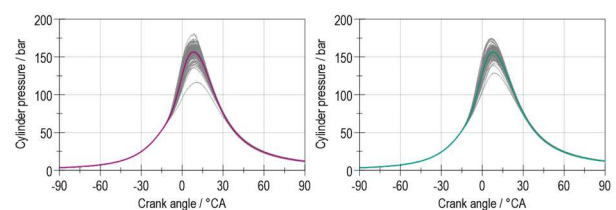


Figure 22. Cylinder pressure over 100 cycles and mean value (coloured). Left: Hydrogen-ammonia combustion at 85 % energetic  $\text{NH}_3$  share. Right: 100 % ammonia combustion.

The COV of IMEP and the indicated efficiency of this comparison can be seen in Figure 23. The efficiency drops by 2 % from 50 % to 48 % with the

100 % ammonia combustion. The cooling effect of the ammonia leads to a lower combustion temperature and thus to a lower efficiency. The combustion stability is better with 100 % ammonia at around 1.9 %.

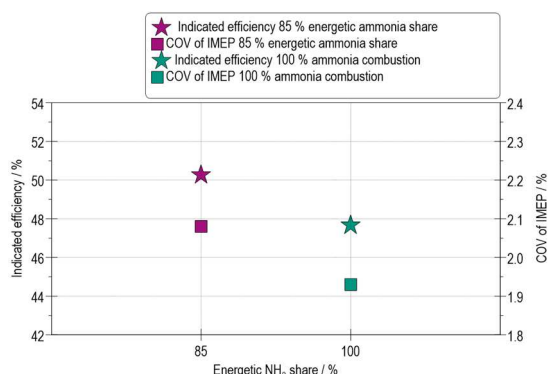


Figure 23. Indicated efficiency and COV of IMEP over the energetic NH<sub>3</sub> share for the H<sub>2</sub>-NH<sub>3</sub> combustion and 100% ammonia combustion at 17 bar IMEP

Summing up it can be said the 100 % ammonia combustion is burning as quick as the hydrogen-ammonia combustion. The efficiency of the 100 % ammonia combustion is a bit lower due to lower temperatures in the combustion chamber at the end of the compression. The key to a successful ammonia SI combustion is high energy in the ignition.

#### 4.4.3 Diesel-Fuel-Ammonia Combustion vs. SI Ammonia-Hydrogen Combustion

In this chapter a diesel-fuel-ammonia combustion process will be compared to a SI hydrogen-ammonia combustion process with the high energy ignition system at 17 bar IMEP. In both combustion processes ammonia is injected in PFI mode. The diesel-fuel is injected directly into the combustion chamber as shown in Figure 24. In the SI combustion process, ammonia and hydrogen are injected in PFI mode, as shown in Figure 8. The measuring point for the charge air temperature is before the ammonia injection. The SI measurement is made at a stoichiometric air-fuel ratio of 1 and the diesel-fuel-ammonia measurement is made with slightly lean air-fuel ratio of 1.1. The goal of this measurements was to achieve the highest possible energetic ammonia share and use the diesel-fuel as pilot fuel.

The important value for a stable diesel-fuel-ammonia combustion is a high compression end temperature which is mainly influenced by the charge air temperature and the evaporation of the ammonia. The better the ammonia is homogenised and in gaseous phase in the combustion chamber, the more stable is the combustion. The high

evaporation energy of the ammonia leads low compression end temperatures, which make it more difficult for the diesel-fuel to ignite the mixture.

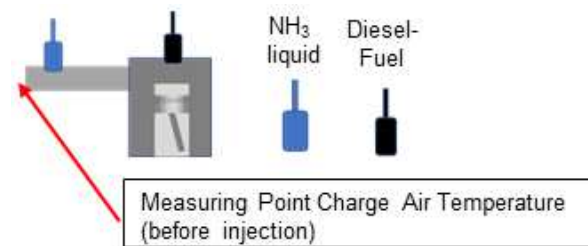


Figure 24. Principle sketch of the engine assembly with diesel-fuel and ammonia injector position

Figure 25 shows the COV of IMEP and the indicated efficiency for the diesel-fuel-ammonia combustion process at different charge air temperatures compared to the SI hydrogen-ammonia combustion. It can be observed that the charge air temperature has an influence on the combustion stability. The higher charge air temperature ensures a better evaporation and homogenization of the ammonia. The compression end temperature increases and with it the ignition capability. This means that a higher charge air temperature increases the possible energy NH<sub>3</sub> share of the combustion process. Increasing the charge air temperature has no negative effects on the diesel-fuel-ammonia combustion process because there is no tendency to knocking, pre-ignition or backfire as it is the case with the hydrogen-ammonia combustion process. There the charge air temperature cannot be increased indefinitely with regard to combustion anomalies.

It has been shown that the diesel-fuel-ammonia combustion process enables an energetic NH<sub>3</sub> share of 97 % for all charge air temperatures. With the SI combustion process, pure ammonia operation is possible. This means that the difference in the energetic NH<sub>3</sub> share is 3%. Both combustion processes are able to burn very high to pure ammonia stably.

The indicated efficiency is slightly increasing with increasing energetic NH<sub>3</sub> share. This is due to a faster burnthrough behaviour of the diesel-fuel-ammonia combustion process. The SI combustion process is not accelerated by the higher energetic ammonia share which can be seen in Figure 29.

Figure 26 shows the cylinder pressure for 100 cycles and their mean value (colored) for the hydrogen-ammonia combustion and diesel-fuel-ammonia combustion at 90 % energetic NH<sub>3</sub> share and 40 °C charge air temperature. It can be observed that the peak pressure is slightly higher for the diesel-fuel-ammonia combustion this due to

the higher air demand caused by the leaner lambda of the diesel-fuel-ammonia combustion. In Figure 26 the kink in the cylinder pressure curve shows the start of burning.

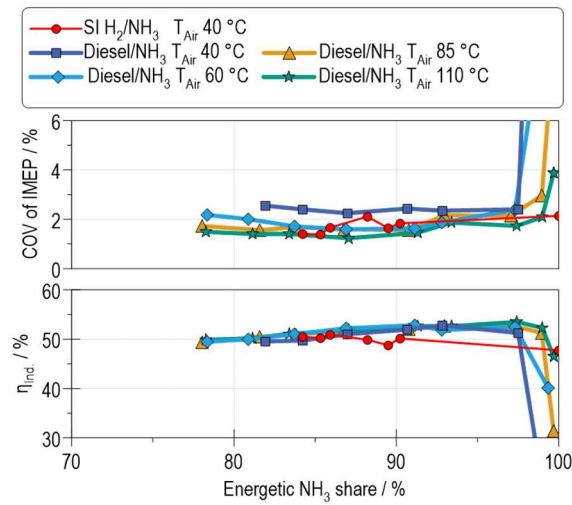


Figure 25. COV of IMEP and Indicated Efficiency over the energetic NH<sub>3</sub> share for diesel-fuel-ammonia combustion at different charge air temperatures and SI hydrogen-ammonia combustion.

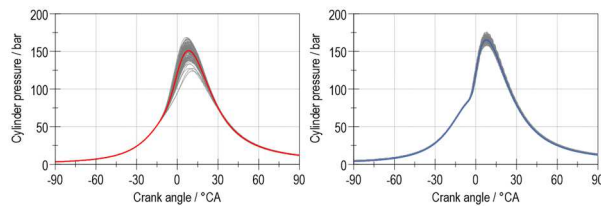


Figure 26. Cylinder pressure over 100 cycles and mean value (coloured) at 17 bar IMEP. Left: SI hydrogen-ammonia combustion at 90 % energetic NH<sub>3</sub> share, T<sub>Air</sub>=40 °C, lambda 1. Right: diesel-fuel-ammonia combustion at 90 % energetic NH<sub>3</sub> share and T<sub>Air</sub>=40 °C, lambda 1.1.

Figure 27 shows the total heating value, the net heat release and the injection timing for the diesel-fuel-ammonia combustion at 90 % energetic NH<sub>3</sub> share for 40 °C and 110 °C. The diesel-fuel-ammonia combustion with an intake temperature of 110 °C has a lower burning delay and a faster burnthrough behaviour.

Figure 28 shows the total heating value, the net heat release and the injection timing for the diesel-fuel-ammonia combustion and hydrogen-ammonia combustion at 90 % energetic NH<sub>3</sub> share. The SI H<sub>2</sub>-NH<sub>3</sub> combustion is somewhat delayed (note advanced ignition timing) and slower, which is reflected in a less pronounced pressure rise and a smoother mfb curve compared to the diesel-fuel-ammonia combustion. The SI H<sub>2</sub>-NH<sub>3</sub> combustion

process burns more slowly until ammonia is converted into hydrogen. In the diesel-fuel-ammonia combustion process, the diesel-fuel is converted very quickly. It ignites everywhere in the combustion chamber at the same time, while the homogeneously distributed hydrogen must first be captured by the flamefront. This leads to a high gradient at the start of the diesel-fuel-ammonia combustion. Once the combustion has completely started, both mfb curves are very similar.

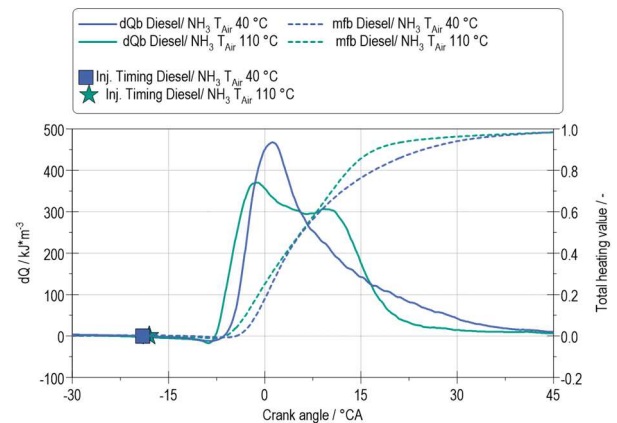


Figure 27. Total heating value, net heat release rate and ignition timing over crank angle for diesel-fuel-ammonia combustion at 17 bar IMEP and 90 % energetic NH<sub>3</sub> share.

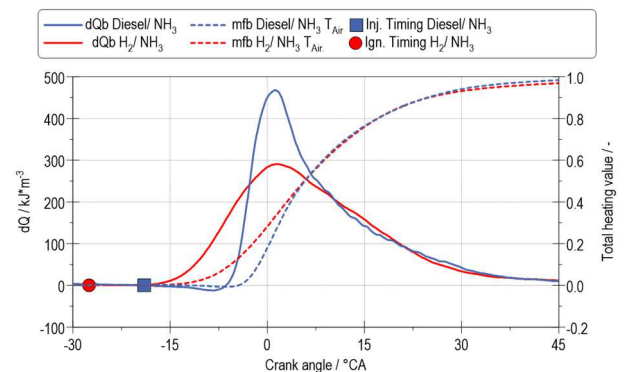


Figure 28. Total heating value, net heat release rate and ignition timing over crank angle for a diesel-fuel-ammonia combustion and a hydrogen-ammonia combustion at 17 bar IMEP, T<sub>Air</sub> = 40 °C and 90 % energetic H<sub>2</sub>/ NH<sub>3</sub> share.

In Figure 29 the influence of the energetic NH<sub>3</sub> share on the burnthrough behaviour can be seen. The increase of the charge air temperature causes a quicker burnthrough of the combustion process. The SI H<sub>2</sub>-NH<sub>3</sub> combustion needs more spark advance but once it is ignited it burns as fast as the comparable diesel-fuel-ammonia combustion. This means the mfb 5 % is significantly earlier for the SI H<sub>2</sub>-NH<sub>3</sub> combustion process so the first phase of ammonia-hydrogen combustion is much faster.

The mfb 50 % is already the same for both combustion processes.

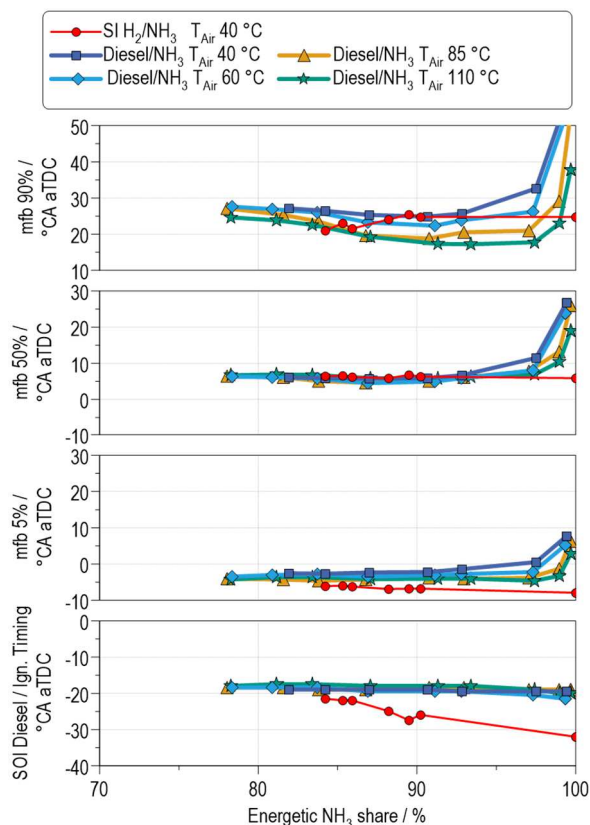


Figure 29. Mfb 90%, mfb 50%, mfb 5% and SOI diesel/Ign. timing over the energetic  $\text{NH}_3$  share for the diesel-fuel-ammonia combustion and hydrogen-ammonia combustion at 17 bar IMEP.

In Figure 30 the  $\text{NH}_3$ ,  $\text{NO}_x$  and unburned  $\text{H}_2$  emissions are plotted vs. the energetic  $\text{NH}_3$  share. The  $\text{NH}_3$  emissions remain stable at around 3000-4000 ppm  $\text{NH}_3$ . The  $\text{NO}_x$  emissions for the diesel-fuel-ammonia combustion process are 1000 ppm above the SI  $\text{H}_2$ - $\text{NH}_3$  combustion process. This is because additional  $\text{NO}_x$  is produced during diesel-ammonia combustion caused by the higher lambda.

The  $\text{NO}_x$  emissions are increasing with increasing energetic  $\text{NH}_3$  share. With SI  $\text{H}_2$ - $\text{NH}_3$  combustion, it has been shown that a slight shift of the air-fuel mixture into rich conditions (lambda 0.98) increases the formation of more hydrogen and less  $\text{NO}_x$  emissions [3]. This explains the fluctuation in  $\text{NO}_x$  emissions in the SI combustion process. A slight deviation of the lambda by 0.02 can lead to this fluctuation. The  $\text{NO}_x$  emissions seem to be on a constantly increasing level for an increase of the energetic  $\text{NH}_3$  share which is similar for both combustion processes.

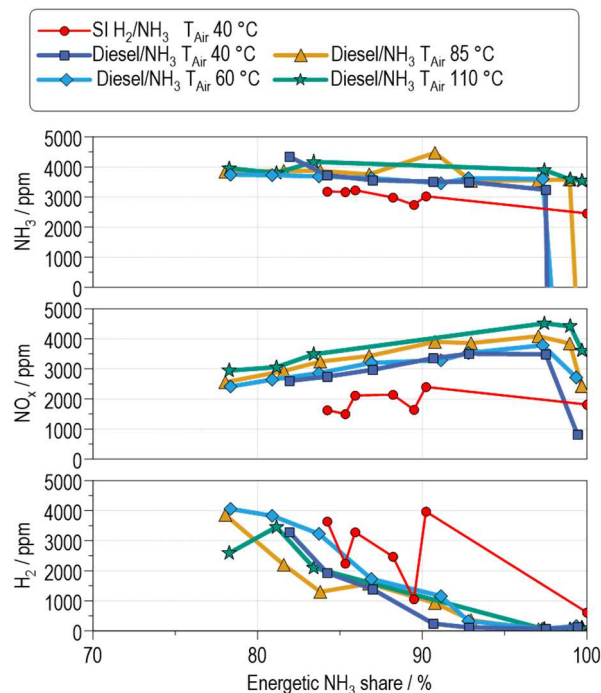


Figure 30.  $\text{NH}_3$ ,  $\text{NO}_x$  and  $\text{H}_2$  emissions over the energetic  $\text{NH}_3$  share for the diesel-fuel-ammonia and hydrogen-ammonia combustion at 17 bar IMEP

Figure 31 shows the CO and  $\text{N}_2\text{O}$  emissions for both combustion processes. It can be observed that the CO emissions for the SI  $\text{H}_2$ - $\text{NH}_3$  combustion are on a very low level around 30 ppm. The measured CO emissions can only be produced by the lubrication oil. The diesel-fuel-ammonia combustion process has decreasing CO emissions for an increasing energetic  $\text{NH}_3$  share. This is due to the lower number of carbon atoms involved in the combustion process and the higher charge air temperature enables a more complete combustion process. The  $\text{N}_2\text{O}$  emissions are on the same level for the diesel-fuel-ammonia combustion and the SI  $\text{H}_2$ - $\text{NH}_3$  combustion.

Summing up it can be said with the diesel-fuel-ammonia combustion and SI  $\text{H}_2$ - $\text{NH}_3$  combustion high energetic  $\text{NH}_3$  shares are possible. With the SI combustion process a stable combustion with 100 % energetic ammonia is possible. The diesel-fuel-ammonia combustion process needs at least 3 % diesel-fuel to provide a stable combustion and it is not sensitive to higher charge air temperatures because there are no combustion anomalies. The  $\text{NO}_x$  and  $\text{NH}_3$  emissions are a higher than the SI combustion process. An exhaust gas aftertreatment system is necessary for both combustion processes.

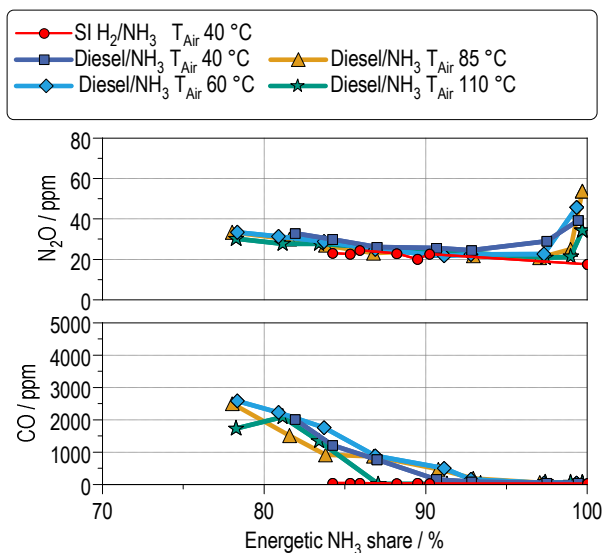


Figure 31. N<sub>2</sub>O and CO emissions over the energetic NH<sub>3</sub> share for the diesel-fuel-ammonia and hydrogen-ammonia combustion at 17 bar IMEP

#### 4.5 Oil Analysis

In addition to the challenges of the combustion process with ammonia, the impact on the lubrication system of the engine is unknown.

Due to the high content of water as a product of the reaction, at first the lubricity therefore depends largely on the capability of the oil to bind water. The specific formation mechanisms during the combustion of ammonia within the engine, continue to lead to an increased concentration of nitrogen oxides in the exhaust gas and blowby. Increased concentrations of water and nitrogen oxides could also lead to an increase in nitric and nitrous acid, with the result that the lubricating oil will be subject to increased acidity. Investigations and analyses are currently being carried out on this aspect in particular.

Furthermore, the interaction between the lube oil and ammonia during the mixture formation process or caused by unburned ammonia in the blow by gas is not known in detail. The enrichment of ammonia in the lubricating oil, particularly for PFI engines, poses a challenge, especially regarding the interaction with copper-based bearings, oil coolers or seals.

Due to these aspects' chemical analysis of the lubricating oil from the SCE research engine were carried out. Over a 150-hour operating time of the research engine with ammonia using a conventional lubricating oil (5W30), a significantly increased copper content as well as a significant drop in the total base number (TBN) in the oil could be determined. The oil had to be changed earlier

than when using conventional fuels. These results are also consistent with other oil analyses performed by the authors on ammonia-fueled combustion engines. All results indicate the need for a more detailed investigation and will lead to the development of new analysis methods as well as to new ammonia-adjusted lubricating oil properties.

## 5 SUMMARY AND OUTLOOK

The need for defossilizing the shipping industry must include solutions for inland waterway vessels as well. For that purpose, an ammonia-fueled cracker-engine-unit is developed within the CAMPFIRE consortium. The focus of this paper was set on the results from the extensive single-cylinder engine test. In addition to the previous work, further important findings were generated, which can be concluded as following:

- The port-fuel-injection of liquid ammonia allows in combination with a high compression ratio diesel-fuel-engine like performance and efficiency values. This can be achieved with a high NH<sub>3</sub> share or even with pure NH<sub>3</sub> engine operation.
- The hydrogen share can be kept constant over the whole load range of the engine. This will allow a cracker operation with low dynamic requirements.
- The available ignition energy at the spark plug is key for an efficient Otto-cycle engine combustion concept.
- The possible energetic NH<sub>3</sub> share for the diesel-fuel-ammonia combustion are on a high level and close to 100%.
- As expected, the NO<sub>x</sub> emissions at engine outlet are quite high. The parallel existing NH<sub>3</sub> slip will allow an effective NO<sub>x</sub> reduction by a passive SCR catalyst in the exhaust passage.
- The laughing gas emissions (N<sub>2</sub>O) are quite low and potentials for further reduction are seen.
- The lube oil is affected by high amounts of NH<sub>3</sub> introduction. This topic will be addressed by further design measures and systematic lube oil investigations.
- Current experiences with the ammonia injection components built the basis for the development of durable injectors.

- The simulation models are in the validation period. Finally, they will allow future system and combustion process optimization.

The next steps are:

- Cracker mounting, basic testing
- Engine manufacturing
- Containerization of cracker and engine with generator
- Installation of cracker and genset container at Campfire Open Innovation Lab (COIL)
- Commissioning and testing of components and complete system
- 1,000-hour system endurance test with component surveys

The final goal is the retrofit of an existing inland water vessel.

## 6 DEFINITIONS, ACRONYMS, ABBREVIATIONS

aTDC	After Top Dead Center
CO	Carbon Monoxide
dQ	Total Heating Value
H <sub>2</sub>	Hydrogen
HP-DI	High pressure direct injection
IMEP	Indicated Mean Effective Pressure
LP-DI	Low pressure direct injection
Mfb	Mass fraction burned
NH <sub>3</sub>	Ammonia
NO <sub>x</sub>	Nitrogen oxides
PFI	Port fuel Injection
SI	Spark Ignited
SCE	Single Cylinder Engine
TBN	Total Base Number
Q <sub>n</sub>	Net Heat Release Rate

## 7 ACKNOWLEDGMENTS

This work was carried out within the CAMPFIRE project of the hydrogen Flagship Project TransHyDE and was funded by the German Federal Ministry for Education and Research.

## 8 REFERENCES AND BIBLIOGRAPHY

- [1] International Maritime Organisation. (7th July of 2023). "International Maritime Organization (IMO) adopts revised strategy to reduce greenhouse gas emissions from international shipping" [Press release]. <https://www.imo.org/en/MediaCentre/PressBriefings/pages/Revised-GHG-reduction-strategy-for-global-shipping-adopted.aspx> (Last accessed on 13.01.2025).
- [2] [www.wir-campfire.de](http://www.wir-campfire.de)
- [3] Braun A., Baufeld T., Bernhardt S., Kubach H., Mohr H., Prehn S.: "Combustion concept for ammonia-fuelled cracker-engine-unit as propulsion system for inland waterway vessels". 8th Rostock Large Engine Symposium. September 12-13th 2024. Rostock Germany; [https://doi.org/10.18453/rosdok\\_id00004630](https://doi.org/10.18453/rosdok_id00004630) (Last accessed on 13.01.2025).
- [4] Braun, A.; Gierenz, N.; Braun, S.; Kubach, H.; Bernhardt, S.; Prehn, S.; Müller, M.; Engelmeier, L.; Fehleemann, L.; Steffen, M.; Baufeld, T.; Neuhaus, G.; Müller, K.; Mohr, H.: „Aspects of ammonia as Green fuel for Propulsion Systems of Inland Water Vessels". Energy Technology, 2024; <https://doi.org/10.1002/ente.202301648> (Last accessed on 13.01.2025).
- [5] Renner, V.; Bialonski, W.: "Technische und wirtschaftliche Konzepte für flußangepaßte Binnenschiffe", Versuchsanstalt für Binnenschiffbau e. V., Duisburg 1701, 2004
- [6] Heinz Herwig: Wärmeübertragung A–Z: Systematische und ausführliche Erläuterungen wichtiger Größen und Konzepte. Springer, 2000, ISBN 3-540-66852-7, S.109.
- [7] Čaika, V. and Dörr, N., "Thermal and Transport Properties of diesel fuel and their Effect on Injection Modelling," SAE Technical Paper 2005-24-054, 2005, <https://doi.org/10.4271/2005-24-054> (Last accessed on 13.01.2025).
- [8] Pessina V, Berni F, Fontanesi S, Stagni A, Mehl M. 2022 Laminar flame speed correlations of ammonia/hydrogen mixtures at high pressure and temperature for combustion modeling applications. Int Journal of hydrogen Energy, 47:25780–25794

[9] Ängeby, J.; Gustafsson, B.; Johnsson, A.: „Zündsteuerungsmodul für Wasserstoffverbrennungsmotoren“. MTZ Motortechnische Zeitschrift. Vol. 84, Nr. 10, S. 48–53, 2023

[10] Braun, A.; Kubach, H.; Braun, S.; Reinbold, M.; Bernhardt, S.; Gierenz, N.; Buchholz, B.; Engelmeier, L.; Fehlemann, L.; Plass, J.; Steffen, M.; Baufeld, T.; Prehn, S.; Mohr, H.: “Development of an ammonia-fueled Cracker-Engine-Unit as propulsion System for Inland Waterway Vessels”, 13th Dessau Gas Engine Conference. May 15-16th 2024. WTZ Roßlau. Dessau Germany

[11] Shin J., Park S., “An ammonia flash break-up model based on bubble dynamics with force and energy analysis on droplet,” fuel 342, 127841 (2023)

## 9 CONTACT

Annalena Braun  
Research Assistant

Postal address:  
KIT - Campus Ost  
Institute of Internal Combustion Engines  
Rintheimer Querallee 2  
76131 Karlsruhe (Germany)

Tel: +49 721 / 608 43637  
E-Mail: Annalena.Braun@kit.edu